

# Accelerated Aging of Elastomeric Composites with Vulcanized Ground Scraps

Larissa N. Carli,<sup>1,2</sup> Otávio Bianchi,<sup>2</sup> Raquel S. Mauler,<sup>2</sup> Janaina S. Crespo<sup>1</sup>

<sup>1</sup>Centro de Ciências Exatas e Tecnologia, Universidade de Caxias do Sul, Rua Francisco Getúlio Vargas, 1130, Caxias do Sul, 95070-560, RS, Brazil

<sup>2</sup>Instituto de Química, Universidade Federal do Rio Grande do Sul, Av. Bento Gonçalves, 9500, Porto Alegre, 91501-970, RS, Brazil

Received 19 February 2010; accepted 26 October 2010

DOI 10.1002/app.33666

Published online 27 July 2011 in Wiley Online Library (wileyonlinelibrary.com).

**ABSTRACT:** The aim of this work is to study the effect of thermal aging on the mechanical, dynamic-mechanical, and chemical properties of SBR (styrene-butadiene rubber) composites filled with SBR industrial rubber scraps. Eight composites with varying proportions (10–80 phr) of the SBR ground scraps (SBR-r) were prepared and subjected to accelerated aging in an air-oven. The composites were evaluated, and the results were compared with a control sample (base formulation with 0 phr of SBR-r), before and after thermal aging. The accelerated aging led to a decrease in the mechanical properties as a result of an increase in the stiffness of the material, related to an increase in the cross-

link density. However, these properties were not affected by the addition of rubber scraps up to 50 phr, either before or after aging. The increase in the glass transition temperature of the composites after aging, measured using dynamic mechanical analysis, confirmed the occurrence of a postcrosslinking process. Fourier transform infrared spectroscopy and crosslink density revealed that the aging mechanism was dependent on the SBR-r content. © 2011 Wiley Periodicals, Inc. *J Appl Polym Sci* 123: 280–285, 2012

**Key words:** rubber; recycling; accelerated aging; mechanical properties; FTIR

## INTRODUCTION

Dienic elastomers are very sensitive to chemical changes when exposed to severe weather conditions due to the presence of double bonds in the main chain, which make them easily subjected to radical attack.<sup>1,2</sup> Aging (oxidation) generally results in dramatic changes of the physical–mechanical properties, such as cracking or loss of tensile strength. These changes may adversely affect the reliability and long-term performance of the materials, limiting their service life time. Thus, aging effects are important factors when considering both cost and quality.<sup>3–7</sup>

The exposure of these materials to oxidizing environments (radiation, high temperatures, weathering, etc.) results in two main phenomena: chain scission and postcrosslinking.<sup>4,8–10</sup> The extent and ratio of these two processes are related to the elastomer type and compounding, temperature, and oxygen concentration.<sup>7</sup> After aging, the elastomeric material softens or stiffens, depending on whether chain scission or crosslinking is more extensive.<sup>9</sup>

The degradation of the main chain creates shorter polymer chains and causes deterioration of the mechanical properties, as compared to properties of the unaged rubber. The increase in the crosslink density decreases the average molar mass of the rubber chain between two successive crosslink points, and the mobility of the chain segment is restricted. Therefore, chain-scission leads to a decrease in the viscosity, whereas postcrosslinking makes the material more rigid. The combination of the two phenomena can result in the formation of microcracks.<sup>6,8,10</sup>

The subjects of accelerated aging and swelling of rubber composites are still open for discussion. Many researchers have studied the thermal aging behavior of conventionally filled rubber,<sup>5,9–13</sup> but data regarding the effect of vulcanized ground scraps on the aging resistance of rubber composites in the literature are limited.<sup>14–16</sup>

The mechanical recycling of vulcanized rubber scraps is a low-cost alternative in the search for the recovery of this kind of industrial solid waste. Recycled vulcanized rubber can serve as a partial replacement for virgin rubber, with sulfur introduced to the ground scrap rubber and the compound subsequently vulcanized.<sup>17</sup> According to Nelson and Kutty,<sup>14</sup> the presence of recycled rubber powder, which is more prone to degradation, lowers the mechanical properties of composites compared to conventional compositions.

Correspondence to: J. S. Crespo (jscrespo@ucs.br).

Contract grant sponsors: CAPES; CNPq; FAPERGS.

In our previous work, SBR composites were prepared and evaluated using vulcanized ground scraps with a composition identical to that of the base formulation, used in the fabrication processes of extruded profiles. Studies of the mechanical properties, such as tensile and tear strength, showed that up to 50 phr of SBR-r can be added without an adverse effect.<sup>18</sup>

In this article, the effect of air-oven accelerated aging on the mechanical, dynamic-mechanical, and chemical properties of SBR composites filled with industrial rubber scraps was studied. The characteristics of the developed compositions with SBR ground scraps (SBR-r composites) were evaluated and compared with the control sample (base formulation with 0 phr of SBR-r), before and after thermal aging.

## MATERIALS AND METHODS

### Materials

The SBR extruded profile scraps used in this study were supplied by Ciaflex Indústria de Borrachas Ltda. (Caxias do Sul, RS, Brazil). Approximately 24 kg of scraps were collected from July 2, 2007 to August 11, 2007, according to ASTM E 300-03, and ground under ambient conditions. The characterization of the powder obtained (SBR-r) was carried out based on currently used techniques.<sup>19–21</sup> The obtained SBR powder (SBR-r) was characterized in our previous work and had a particle size distribution in the range of 28–35 mesh. The partial composition of the scraps, obtained by thermogravimetric analysis, was as follows: 27.6% SBR, 34.1% CaCO<sub>3</sub>, 24.1% oil, 12.1% carbon black, and 2.1% other additives.<sup>18</sup>

### Preparation of SBR-r composites

Eight composites were prepared by incorporating SBR-r (varying from 10 to 80 phr) in a control sample that had an identical composition to the extruded profile scraps supplied by Ciaflex Indústria de Borrachas Ltda. A laboratory size open two-roll mill (MH, model MH-600C) was used, according to ASTM D 3182-06. A control sample (base formulation with 0 phr of SBR-r) was also analyzed during every experiment. The compounding ingredients such as sulfur and various accelerators were the same and proportional to the neat SBR in all of the composites and the control sample.

The specimens for the physical–mechanical analysis were made by compression molding at 160°C under a pressure of 7.5 MPa, in a Shultz electrically heated hydraulic press for the optimum cure time,  $t_{90}$ ,<sup>18</sup> which was determined by an oscillating disk rheometer (ODR) Tech Pro-Rheotech OD+, according to ASTM D 2084-06.

### Evaluation of mechanical properties

For the tensile tests, dumbbell-shaped samples (Die D) were cut from the molded sheets according to ASTM D 412-06a. A tear test was carried out according to ASTM D 624-00 with Die C-shaped test pieces. The tests were performed at a crosshead speed of 500 mm min<sup>-1</sup>, with an EMIC DL-3000 instrument. Five specimens were analyzed, and the average and standard deviation were calculated.

A Shore A Teclock durometer, model GS709, was used to measure hardness in accordance with ASTM D 2240-05. The compression set test was carried out at 23 and 70°C for 22 h according to ASTM D 395B-03. Abrasion resistance was measured using Maqtest equipment according to ASTM D 5963-04.

The tests were carried out after 40 h of conditioning the specimens at 23°C ± 2°C and a relative humidity of 50% ± 5%.

### Dynamic mechanical analysis

Dynamical experiments were carried out in a DMA Q800 (TA Instruments) using single cantilever geometry. The experiment was conducted within the linear viscoelastic region using a small amplitude (0.1%). The heating rate was fixed at 3°C min<sup>-1</sup>, and the frequency was set at 1 Hz for all samples. Rectangular-shaped samples (30 × 12 × 2 mm<sup>3</sup>) were used in these experiments. The viscoelastic behaviors of the samples were assessed in terms of loss tangent (tan δ) and storage modulus ( $E'$ ), within the temperature range of –90–30°C.

### Fourier transform infrared spectroscopy

The chemical changes upon aging were followed by ATR-FTIR (Attenuated Total Reflectance) with 64 scans and a resolution of 2 cm<sup>-1</sup>, in a Nicolet 6700 spectrophotometer. Both the material surface and an area near the middle of the sample thickness (at a depth of 1 mm) were analyzed, before and after aging.

### Crosslink density

The chemical characterization of the samples involved the determination of crosslink density. The crosslink density [ $X$ ] was obtained by a swelling experiment, using the Flory-Rehner equation<sup>22</sup> with the Kraus correction,<sup>23</sup> based on the fact that vulcanized rubbers swell to equilibrium degrees when immersed in liquids.<sup>19</sup> Samples with approximate dimensions of 20 × 20 × 2 mm<sup>3</sup> were immersed in *n*-heptane in the dark at 23°C ± 2°C for 7 days.

### Accelerated aging methodology

Accelerated aging of the SBR-r composites was performed in a forced air circulating oven (Erzinger, model 90/65/70) at 70°C for 170 h, according to ASTM D 573-04. The tests with aged specimens were carried out after 40 h of conditioning at 23°C ± 2°C and a relative humidity of 50% ± 5% to obtain thermal equilibrium before measuring their physical properties.

The properties of the SBR-r composites were determined in the same manner as described above, and the results were compared with the corresponding unaged samples. The property retention values were determined using eq. (1):

$$\text{Property retention value} = \left( \frac{P}{P_0} \right) \cdot 100 \quad (1)$$

where  $P_0$  and  $P$  are the properties of the SBR-r composites before and after the accelerated aging process, respectively. The properties of the unaged samples were presented in our previous work.<sup>18</sup>

## RESULTS AND DISCUSSION

### Mechanical properties

In our previous paper,<sup>18</sup> the rheometric, mechanical, and morphological characteristics of the unaged SBR-r composites were evaluated. The effect of the accelerated aging process on the mechanical behavior of these composites is presented in Figure 1, which shows the property retention values of tensile strength, elongation at break, and tear strength [Fig. 1(a)]; and Shore A hardness, compression set, and abrasion loss [Fig. 1(b)].

A slight increase in the tensile strength values was observed for composites with a SBR-r content between 30 and 60 phr. For the other samples, aging process resulted in a decrease in the retention values. A similar trend was also observed for tear strength. In all cases, the value of the tear strength was reduced after aging.

Aging also caused a decrease in the elongation at break values, as a result of the reduced elasticity of elastomeric matrix. The decrease in the mechanical properties can be primarily attributed to the increase in elastomeric stiffness.<sup>9,24</sup> The increase in stiffness arises from the increase in the crosslink density via a post cure process, which may exceed the optimum value and cause networks to become too dense.<sup>11,25</sup> These results are evidenced by the crosslink density values given in Figure 6 and discussed later.

After accelerated aging, an increase in the Shore A hardness was observed. The increase arises because the polymer chains cannot explore different configura-

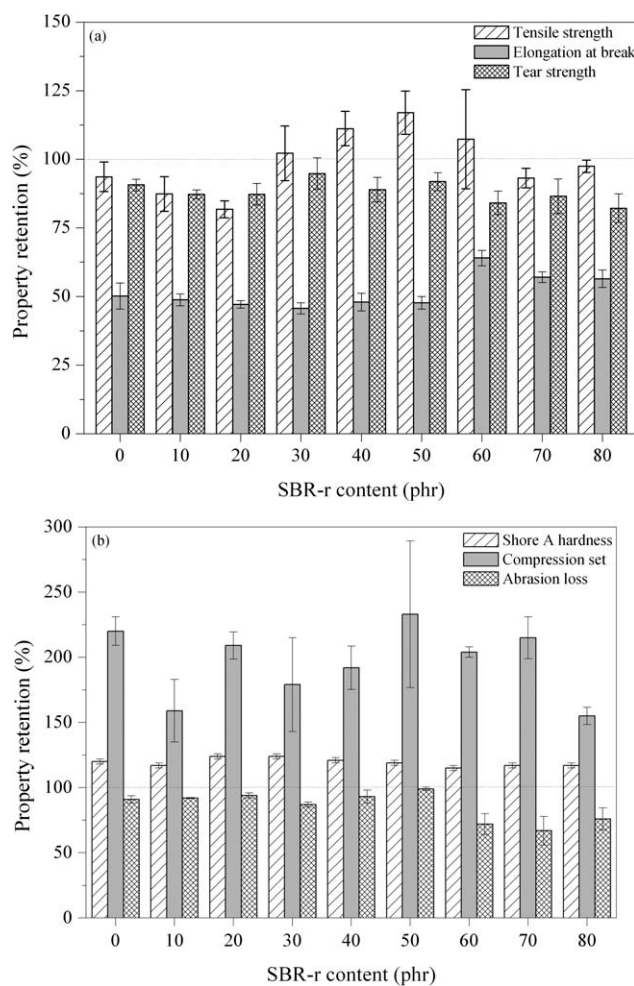


**Figure 1** Property retention values of the SBR-r composites exposed to accelerated aging, relative to the properties before aging (the dotted line corresponds to 100%). (a) tensile strength, elongation at break, and tear strength and (b) Shore A hardness, compression set, and abrasion loss.

tions during constraint and are therefore less flexible.<sup>6</sup> This can be also attributed to the formation of additional crosslinks via a post curing process, reducing the mobility of rubber chains.<sup>11,24</sup>

The aged SBR-r composites showed a marked difference in compression set values at 70°C for 22 h in comparison to the unaged samples at 23°C. A higher percent of the compression set means a permanent deformation of the rubber in a compressed form.<sup>26</sup> Therefore, the increase in the compression set values can be attributed to the reduced elasticity of the elastomeric matrix, which facilitates irreversible flow under stress.<sup>14</sup>

For the abrasion tests, the results revealed that the aging of the SBR-r composites increased the abrasion resistance of the materials, independent of the SBR-r content. Similar studies<sup>15,27</sup> reported that a greater crosslink density, higher hardness, and modulus values give rise to the enhancement of the abrasion resistance of rubber.

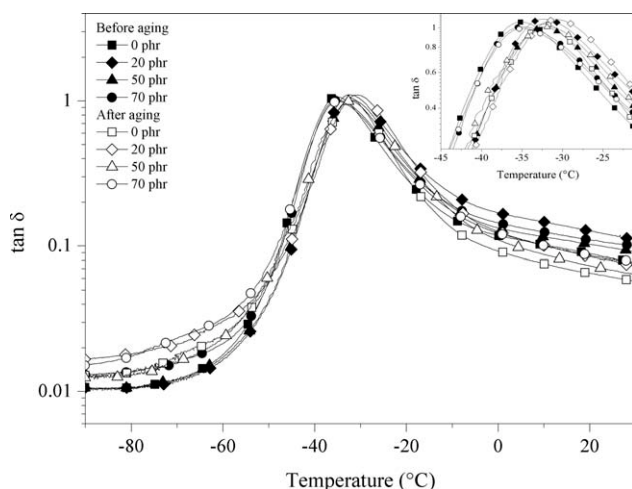


**Figure 2** Effect of SBR-r content and accelerated aging on the  $\tan \delta$  of SBR-r composites with respect to temperature.

### Dynamic mechanical analysis

Figure 2 shows the loss tangent ( $\tan \delta$ ) curves of SBR-r composites. In this study, the maximum value of the  $\tan \delta$  is attributed the glass transition temperature ( $T_g$ ) of the composites. The  $\tan \delta$  represents the damping in the system or the energy loss per cycle, and it is defined by  $\tan \delta = E'/E''$ , where  $E'$  is the storage modulus due to the stored elastic energy in the material and  $E''$  is the loss modulus due to viscous dissipation.<sup>28,29</sup>

It can be seen that  $\tan \delta$  values of the unaged SBR-r composites peak near  $-45$  and  $-15^\circ\text{C}$ , which is known as the glassy (rigid) to rubbery state transition region. After thermal exposure,  $\tan \delta$  values shifted to slightly higher temperatures. The increase in the glass transition temperature (see detail in Fig. 2) can be associated with the higher restriction on chain mobility as a result of the increased crosslink density after aging, as showed in Figure 6 and discussed below.

The increase in the  $T_g$  values was more pronounced for lower SBR-r contents. Contrary to the results reported by Nelson and Kutty,<sup>14</sup> this result indicates that the neat rubber is more sensitive to aging effects than the rubber scraps. The same trend was observed in the ATR-FTIR analysis, as discussed below.

A comparison between the storage modulus for SBR-r composites, before and after aging, is shown in Figure 3. The addition of scrap rubber to the SBR matrix resulted in an increase of the storage modulus values in the elastic plateau region, since the rubber residue is already crosslinked. The elastic plateau region in rubber materials is typically affected by crosslink linkages and by their extension.<sup>22</sup> The increase in rigidity caused by radical attack and their recombination after accelerated aging contributed more significantly to the elastic

component ( $E'$ ) of the materials. As a consequence, a reduction in the chain mobility after aging resulted in an increase in the elastic component for all samples, corroborating the mechanical results.

The  $E'$  values, which were higher than those obtained before aging, can be related to more than just the increased stiffness of the elastomeric matrix. According to the literature, higher  $E'$  values can also be indicative of a good interaction between the particles and the elastomeric matrix.<sup>5,30</sup> These results suggest that in this case, the aging process did not contribute to the detachment of SBR-r particles from SBR matrix, which can be related to the improvement in the abrasion resistance observed after thermal exposure [Fig. 1(b)].

### ATR-FTIR results

The ATR-FTIR analysis was used to compare the effect of accelerated aging on the chemical structure of the SBR-r composites that were exposed to thermal aging. Figure 4 shows the ATR-FTIR spectra of the control sample at the surface (upper spectrum) and interior ( $\sim 1$  mm—lower spectrum), before and after the accelerated aging process [Fig. 4(a,b), respectively].

The peaks in the region between  $2954$  and  $2849\text{ cm}^{-1}$ , as well as the peaks between  $1472$  and  $1393\text{ cm}^{-1}$ , observed in Figure 4(a,b), are assigned to the  $\text{CH}_3$  and  $\text{CH}_2$  bonds, either at the surface or in the interior of the samples, relative to the rubber structure. The peaks at  $1736$  and  $1728\text{ cm}^{-1}$ , attributed to the carbon-oxygen double bond stretching vibrations, were observed only at the surface of the samples, either before or after accelerated aging. The absence of these peaks in the interior of the composites indicates that this oxidative effect observed

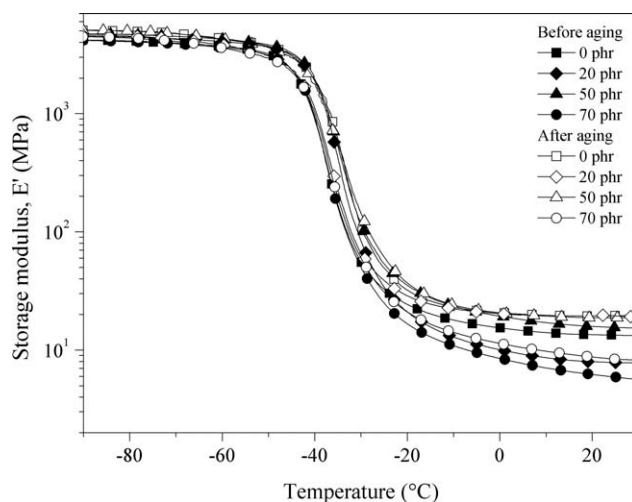


**Figure 3** Effect of SBR-r content and accelerated aging on the storage modulus of SBR-r composites with respect to temperature.

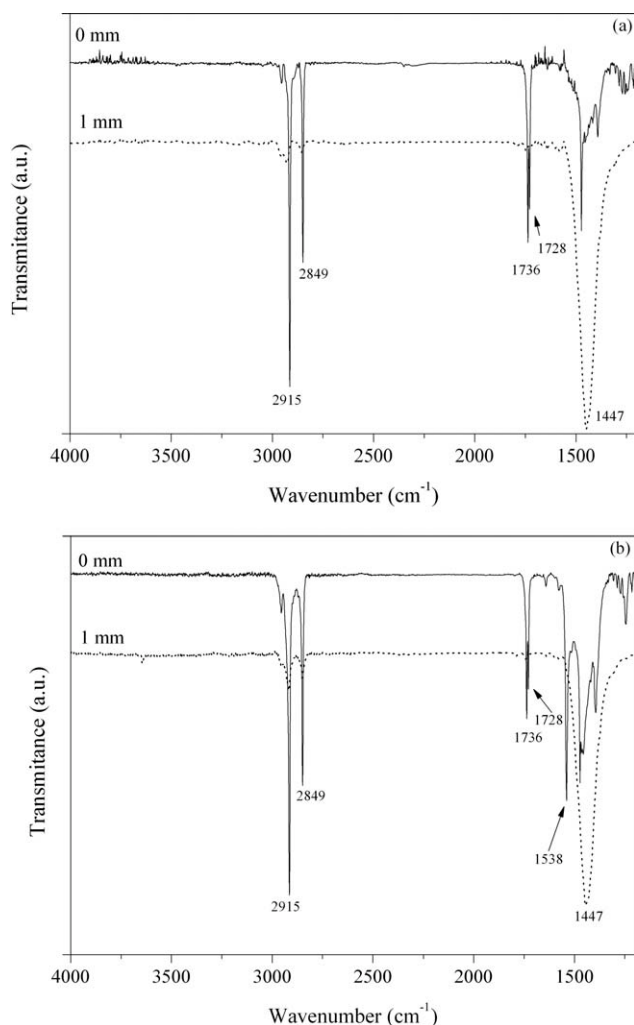


**Figure 4** ATR-FTIR spectra of the control sample (a) before and (b) after accelerated aging. Upper spectrum represents analysis at the surface (0 mm) and the lower spectrum, the interior (1 mm) of the control sample.

in the surface can be also due to the compression molding process of the samples.

The presence of a peak at  $1538\text{ cm}^{-1}$  in the aged sample, assigned to the  $\text{COO}^-$  stretching, indicated the presence of thermo-oxidative degradation of the SBR-r composites at the surface. Several studies<sup>3,31–33</sup> reported the formation of carboxylate group as the main oxidation product on the material surface. Radical attacks, in the presence of  $\text{O}_2$ , lead to the formation of several types of oxygenated species such as alcohols, peroxides, and other carbonyl functions.<sup>1</sup> According to Delor-Jestin et al.,<sup>33</sup> the carboxylic acids are converted into zinc carboxylates, as an effect of the presence of zinc oxide in the formulation. Therefore, the changes in chemical structure can be attributed to an oxidation process taking place at the surface of the samples.

There were no observed changes in the characteristic infrared absorptions in the interior of the

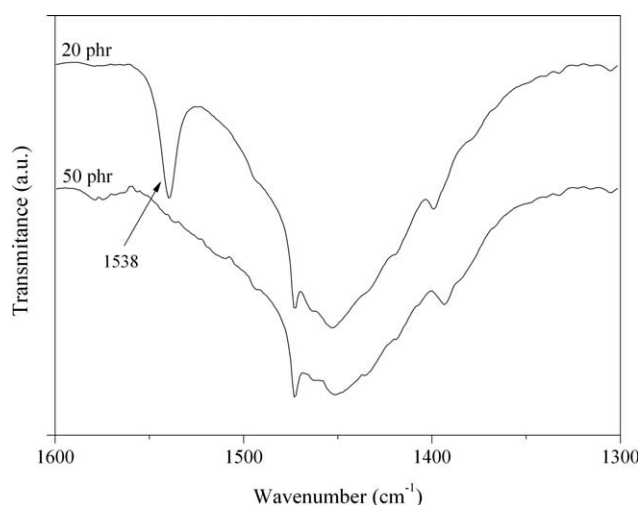
samples after thermal aging. The absence of oxygenated compounds in the interior of the aged samples indicates that the aging process occurred from the SBR surface and then can be propagated to its inner body at longer times of aging.<sup>12,34</sup>

Figure 5 shows the ATR-FTIR spectra taken at the surface of composite specimens with 20 and 50 phr of SBR-r, after accelerated aging. For the lower SBR-r content, the oxidation mechanism took place, evidenced by the peak at  $1538\text{ cm}^{-1}$ . As described above, the changes in chemical structure can be attributed to the formation of carboxylates. For composites with higher SBR-r contents, chain scission and crosslinking are the main effects of thermal aging, evidenced by the absence of peaks related to carbonyl groups and supported by crosslink density results. The rubber scraps were already vulcanized and exposed to thermal aging during the grinding process, which made them less susceptible to oxidation.

Therefore, for lower SBR-r content (up to 20 phr), both aging effects (oxidation of material surface and crosslink formation) can ultimately decrease the mechanical properties of the rubber material.<sup>12</sup> For higher SBR-r content, the increase of the crosslink density is the main effect contributing for the aging of the SBR-r composites. These results corroborate the property retention values of tensile and tear strength between 30 and 60 phr.

### Crosslink density

The incorporation of rubber scraps did not affect the crosslink density, either before or after aging, as shown in Figure 6. The crosslink density of the control sample before aging was determined to be  $1.13 \times 10^{-4}\text{ mol cm}^{-3}$ . During the aging process,



**Figure 5** ATR-FTIR spectra ( $1600\text{--}1300\text{ cm}^{-1}$ ) of the surface of composites with 20 and 50 phr of SBR-r after accelerated aging.

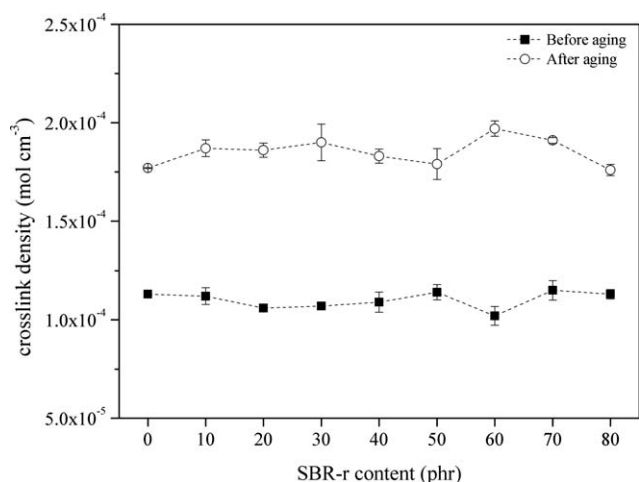


**Figure 6** Crosslink density of SBR-r composites, before and after aging.

residual curing occurred and the crosslink density increased to  $1.77 \times 10^{-4} \text{ mol cm}^{-3}$ . The same trend was observed for all of the SBR-r composites. This result corroborated the decreased mechanical properties after accelerated aging, confirming the reduction in the elasticity of the elastomeric matrix with the exposure of the material to elevated temperatures.

There was a clear increase in the crosslink density after accelerated aging for composites with SBR-r contents above 60 phr. This result agrees with the ATR-FTIR analysis, which indicated that the aging mechanisms for composites with higher SBR-r contents were predominantly chain scission and crosslink formation.

## CONCLUSIONS

Mechanical and physical properties of composite materials were tested before and after an accelerated aging treatment to determine their aging resistance. As a general trend, thermal aging caused a reduction of the mechanical properties. From the results above, it is evident that the aging of SBR-r composites was dependent on the content of vulcanized ground rubber scraps. The surface oxidation was only observed in the composites with lower SBR-r content. For the composites with higher amounts of SBR-r, the degradation of the material was a result of main chain scission and crosslink formation, related to the great quantity of previously aged material. This behavior was evidenced by ATR-FTIR results and measurements of the crosslink density.

The authors are grateful to Ciaflex Indústria de Borrachas Ltda. for supplying the SBR rubber scraps, additives, and the control sample.

## References

- Bussière, P. O.; Gardette, J. L.; Lacoste, J.; Baba, M. *Polym Degrad Stab* 2005, 88, 182.
- Radhakrishnan, C. K.; Alex, R.; Unnikrishnan, G. *Polym Degrad Stab* 2006, 91, 902.
- Delor, F.; Barrois-Oudin, N.; Duteurtre, X.; Cardinet, C.; Lemaire, J.; Lacoste, J. *Polym Degrad Stab* 1998, 62, 395.
- Ngolemasango, F. E.; Bennett, M.; Clarke, J. *J Appl Polym Sci* 2008, 110, 348.
- Escócio, V. A.; Martins, A. F.; Visconte, L. L. Y.; Nunes, R. C. R. *Polímeros Ciênc Tecnol* 2003, 13, 130.
- Tomer, N. S.; Delor-Jestin, F.; Singh, R. P.; Lacoste, J. *Polym Degrad Stab* 2007, 92, 457.
- Bauer, D. R.; Baldwin, J. M.; Ellwood, K. R. *Polym Degrad Stab* 2007, 92, 110.
- Lucas, P.; Baba, M.; Lacoste, J.; Gardette, J. L. *Polym Degrad Stab* 2002, 76, 449.
- Hamed, G. R.; Zhao, J. *Rubber Chem Technol* 1999, 72, 721.
- Ngolemasango, F. E.; Bennett, M.; Clarke, J. *J Appl Polym Sci* 2006, 102, 3732.
- Rattanasom, N.; Prasertsri, S. *Polym Test* 2009, 28, 270.
- Mostafa, A.; Abouel-Kasem, A.; Bayoumi, M. R.; El-Sebaie, M. G. *Mater Des* 2009, 30, 791.
- Azura, A. R.; Ghazali, S.; Mariatti, M. *J Appl Polym Sci* 2008, 110, 747.
- Nelson, P. A.; Kutty, S. K. N. *Prog Rubber Plast Technol* 2002, 18, 85.
- Rattanasom, N.; Poonsuk, A.; Makmoon, T. *Polym Test* 2005, 24, 728.
- Zanchet, A.; Carli, L. N.; Giovanela, M.; Crespo, J. S.; Scuracchio, C. H.; Nunes, R. C. R. *J Elastom Plast* 2009, 41, 497.
- Zanchet, A.; Dal'Acqua, N.; Weber, T.; Crespo, J. S.; Brandalise, R. N.; Nunes, R. C. R. *Polímeros Ciênc Tecnol* 2007, 17, 23.
- Carli, L. N.; Boniatti, R.; Teixeira, C. E.; Nunes, R. C. R.; Crespo, J. S. *Mater Sci Eng C* 2009, 29, 383.
- Bilgili, E.; Arastoopour, H.; Bernstein, B. *Powder Technol* 2001, 115, 277.
- Weber, T.; Zanchet, A.; Crespo, J. S.; Brandalise, R. N.; Nunes, R. C. R. *J Elastom Plast* 2008, 40, 147.
- Massarotto, M.; Crespo, J. S.; Zattera, A. J.; Zeni, M. *Mater Res* 2008, 11, 85.
- Flory, P. J. *Principles of Polymer Chemistry*; Cornell University: New York, 1953.
- Kraus, G. J. *J Appl Polym Sci* 1963, 7, 861.
- Nair, T. M.; Kumaran, M. G.; Unnikrishnan, G.; Kunchandy, S. *J Appl Polym Sci* 2008, 107, 2923.
- Jacob, C.; De, P. P.; Bhowmick, A. K.; De, S. K. *J Appl Polym Sci* 2001, 82, 3293.
- Choi, S.-S.; Han, D.-H. *Thermochim Acta* 2009, 490, 8.
- Maridass, B.; Gupta, B. R. *J Elastom Plast* 2006, 38, 211.
- Ferry, D. *Viscoelastic Properties of Polymers*; Wiley: New York, 1980.
- Menard, K. P. *Dynamic Mechanical Analysis—A Practical Introduction*; CRC Press: Florida, 1999.
- Kumnuantip, C.; Sombatsompop, N. *Mater Lett* 2003, 57, 3167.
- Zhao, Q.; Li, X.; Gao, J. *Polym Degrad Stab* 2007, 92, 1841.
- Zhao, Q.; Li, X.; Gao, J. *Polym Degrad Stab* 2009, 94, 339.
- Delor-Jestin, F.; Lacoste, J.; Barrois-Oudin, N.; Cardinet, C.; Lemaire, J. *Polym Degrad Stab* 2000, 67, 469.
- Brown, R. P.; Soulagnet, G. *Polym Test* 2001, 20, 295.